Electrostatic Drift Instabilities in a Field Reversed Configuration

Shu-ying SUN and Hua-sheng XIE
xiehuasheng@enn.cn, huashengxie@gmail.com

Fusion Research Institute, ENN Group, Langfang, Hebei, 065001, China

With: Yang Li, Bin Chen, Jiang Zhu (FRI-ENN), Yi Zhang (PKU)

YP11.00022

60th Annual Meeting of the APS Division of Plasma Physics,

Nov.5-9, 2018, Portland, Oregon, 97204, the USA

1. Motivation & Background **Motivations**

Advantages of the Field reversed configuration (FRC):

- ✓ high-β
- ✓ large-orbit effects
- ✓ natural divertor
- ✓ Simple structure

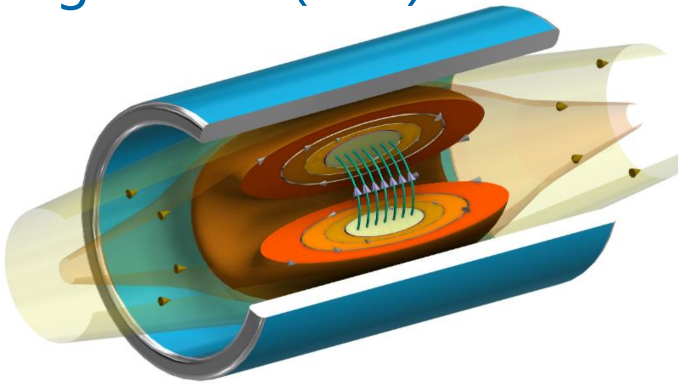

Schematic view of a FRC

(Figure from Y. M. Yang, FRI-ENN)

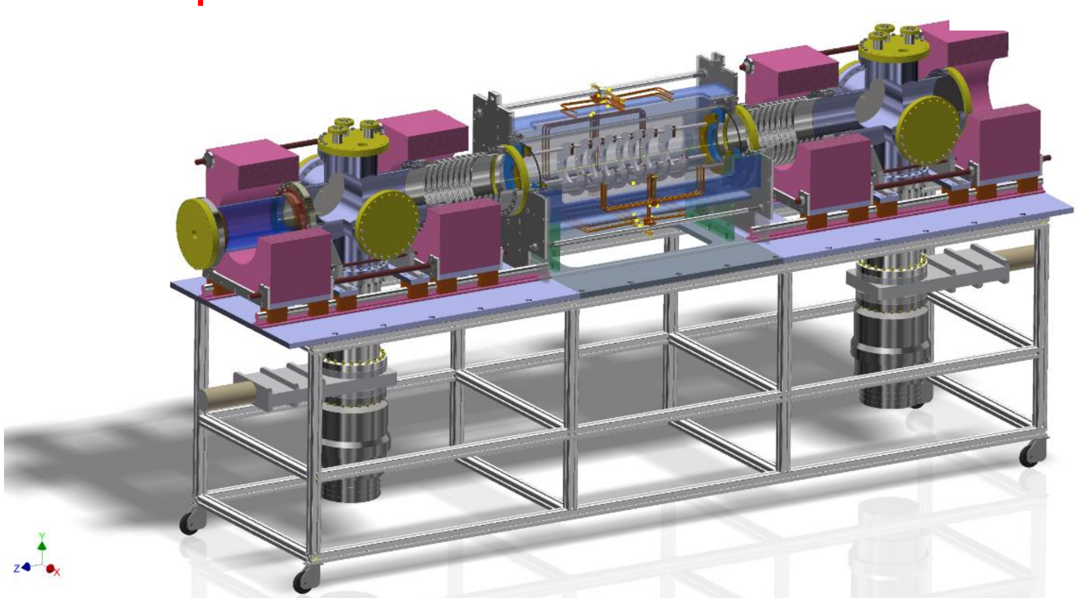

ENN's first FRC device EFRC-0

Recent FRC devices:

- ✓ PFRC in PPPL
- ✓ C-2U and C-2W in TriAlpha Energy
- ✓ KMAX in USTC

1. Motivation & Background   Backgrounds

- ✓ Confinement of a plasma in a FRC for over 10ms achieved.
  Gota et al, *NF.* 2017
- ✓ Suppressed ion-scale turbulence in a hot high-β plasma observed.
  Schmitz et al, *Nat. Comm.* 2016
- ✓ Gyro-kinetic simulations based on these experiments shows the drift-wave instabilities.
  Fulton et al, *PoP.* 2016, 2016a, Lau et al, *PoP*. 2017

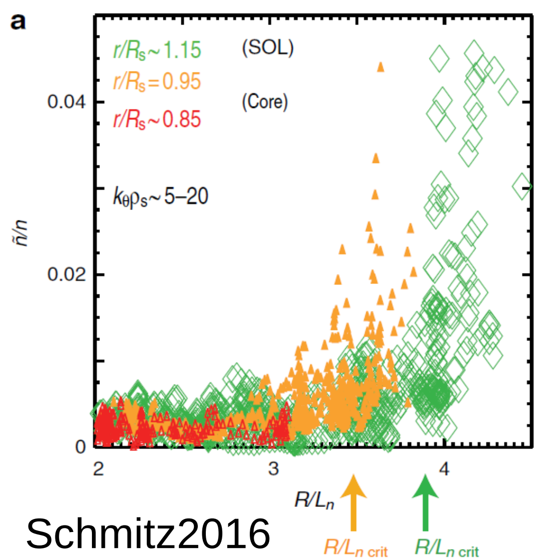

Schmitz2016

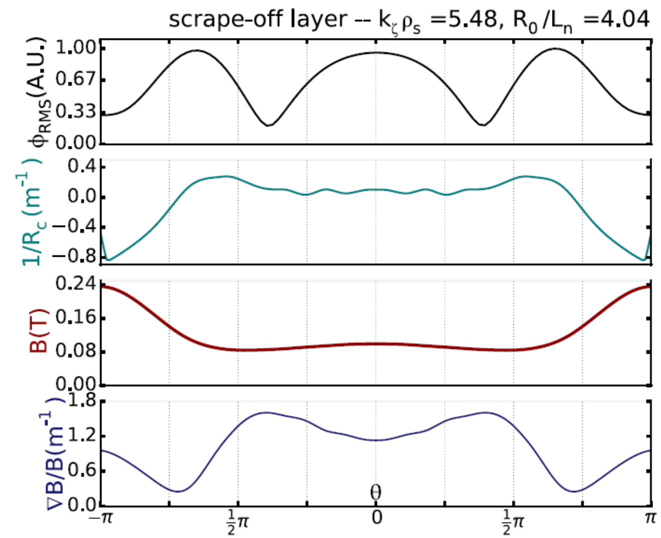

Fulton2016a

Density perturbation is high in SOL region but low in core region of C-2U.

Simulation by GTC code shows drift wave structure in SOL region of C-2U.

3. Gyro-kinetic Model 1D equation system

•1D linear closed equations [H. XIE, *PoP*, 2017; H. XIE, *PoP*, 2017a]

$$f_s = -\frac{q_s \Phi}{T_s}\frac{\partial F_0^s}{\partial \varepsilon} + J_0(k_\perp \rho_s) h_s$$

$$(\omega - \omega_{Ds} + i v_\| \partial_\|) h_s = -(\omega - \omega_{*s}) q_s \Phi \frac{\partial F_0^s}{\partial \varepsilon} J_0(k_\perp \rho_s)$$

$$\sum_s \int f_s dv^3 = 0$$

where, $s = i, e$ is particle species, f_s the perturbed distribution function, Φ the electric potential, J_0 the Bessel function, $\varepsilon = m_s v^2/2$, ρ_s the Larmor radius, ω_{*s} the diamagnetic drift frequency, ω_{Ds} the magnetic drift frequency.

3. Gyro-kinetic Model normalized equations

Adopt flux coordinates (ψ,ξ,φ) of a FRC, $\boldsymbol{B}=\nabla\psi\times\nabla\zeta$.

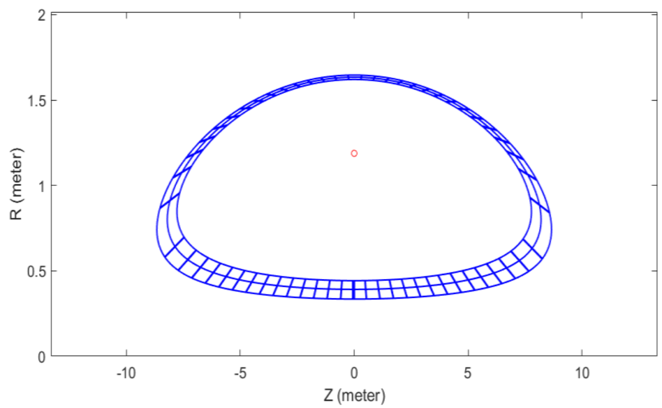

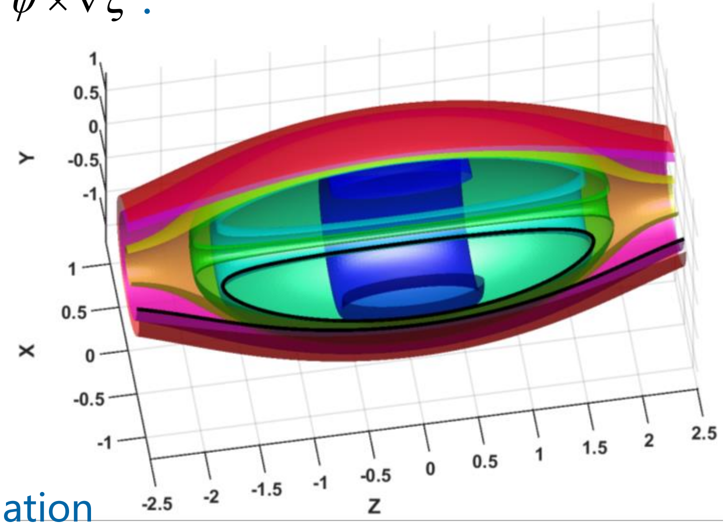

The normalized gyro-kinetic system for particle simulation

$$\frac{d\xi}{dt}=\frac{v_{\parallel}}{\kappa(\xi)}$$

$$\frac{dw}{dt}=-i\omega_{Ds}w-i(\omega_{Ds}-\omega_{*s})\frac{q_s\Phi}{T_s}J_0-\frac{v_{\parallel}}{\kappa(\xi)}\frac{q_s}{T_s}[J_0\frac{\partial\Phi}{\partial\xi}-J_1\Phi\frac{\partial(k_{\perp}\rho_s)}{\partial\xi}]$$

$$[1-\Gamma_0(b_i)+\frac{1}{\tau_e}-\frac{1}{\tau_e}\Gamma_0(b_e)]\Phi=\int(J_{0,i}g_i-J_{0,e}g_e)dv^3$$

To avoid the $\pm v_{\parallel}$ of treating the turning point, we add a new equation to calculate $\pm v_{\parallel}$

$$\frac{dv_{\parallel}}{dt}=-\frac{v_{\parallel}^2}{2\kappa}\frac{dB}{d\xi}$$

where, $w=g/F_0$ is particle weight, $\Gamma_0(b_s)=e^{-b_s}I_0(b_s)$, $b_s=(k_{\perp}\rho_{ts})^2$ $\tau_e=T_e/T_i$

4. Linear 0D dispersion relation

Dispersion relation in 0D limit,

$$D(\omega,k)=\sum_s \frac{1}{T_s}\left\{1-\int dv^3\frac{\omega-\omega_{*s}}{\omega-k_\parallel v_\parallel-\omega_{Ds}}J_0^2(k_\perp\rho_s)F_0^s\right\}=0$$

For simplicity, let $k_\parallel=0$ and $k_\psi=0$, i.e., $k_\perp=k_\varphi$.

With Maxwellian distribution F_M

$$D(\omega,k)=\sum_s \frac{1}{T_s}\left\{1-\frac{1}{\sqrt{2\pi}}\int\frac{\omega-\omega_{*s}}{\omega-k_\parallel v_\parallel-\omega_{Ds}}J_0^2(k_\perp\rho_s)\exp\left(-\frac{v^2}{2v_{ts}^2}\right)\frac{v_\perp}{v_{ts}}d\frac{v_\perp}{v_{ts}}d\frac{v_\parallel}{v_{ts}}\right\}=0$$

Where

$$\omega_{*s}=\omega_{s0}\left[L_n^{-1}+L_T^{-1}\left(\frac{v^2}{2v_{ts}^2}-\frac{3}{2}\right)\right]\qquad \omega_{s0}=k_\perp T_s q_i/q_s T_i\qquad L_n^{-1}=B_0R_0^2\frac{\partial\ln n}{\partial\psi}\qquad L_T^{-1}=B_0R_0^2\frac{\partial\ln T}{\partial\psi}$$

$$\omega_{Ds}=\frac{\omega_{s0}}{rB}\left(c_0\frac{v_\parallel^2}{v_{ts}^2}+\frac{g_0}{2}\frac{v_\perp^2}{v_{ts}^2}\right)\qquad c_0=R_0(\nabla\times\boldsymbol{b})\cdot\boldsymbol{e}_\varphi\qquad g_0=R_0(\boldsymbol{b}\times\nabla\ln B)\cdot\boldsymbol{e}_\varphi$$

Note: without losing the generality, the quantities above have been normalized by R_0, B_0 m_i, q_i, T_i, v_{ti}

4. Scan profile gradient L_n^{-1} and L_T^{-1}

$$m_i / m_e = 3672,\ \tau = 0.2,\ c_0 = -1.164,\ g_0 = -1.164,\ k_\perp \tilde{\rho}_i = 1.0,\ k_\parallel R_0 = 0.0$$

Solid: first branch; dash: second branch

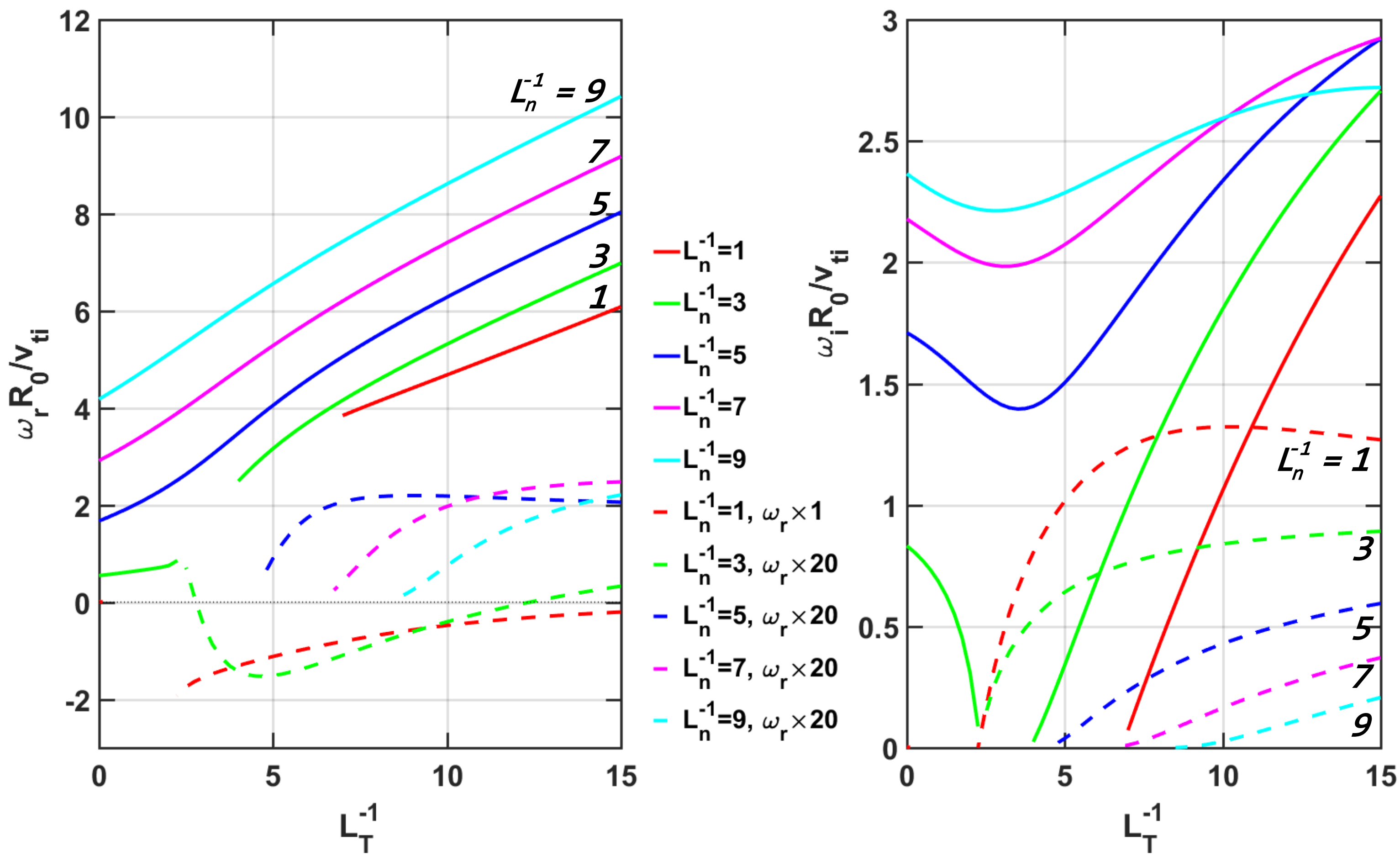

Two unstable branches. Increase of temperature gradient leads to the growth rate increase of linear drift instability.

4. Scan c_0 and g_0

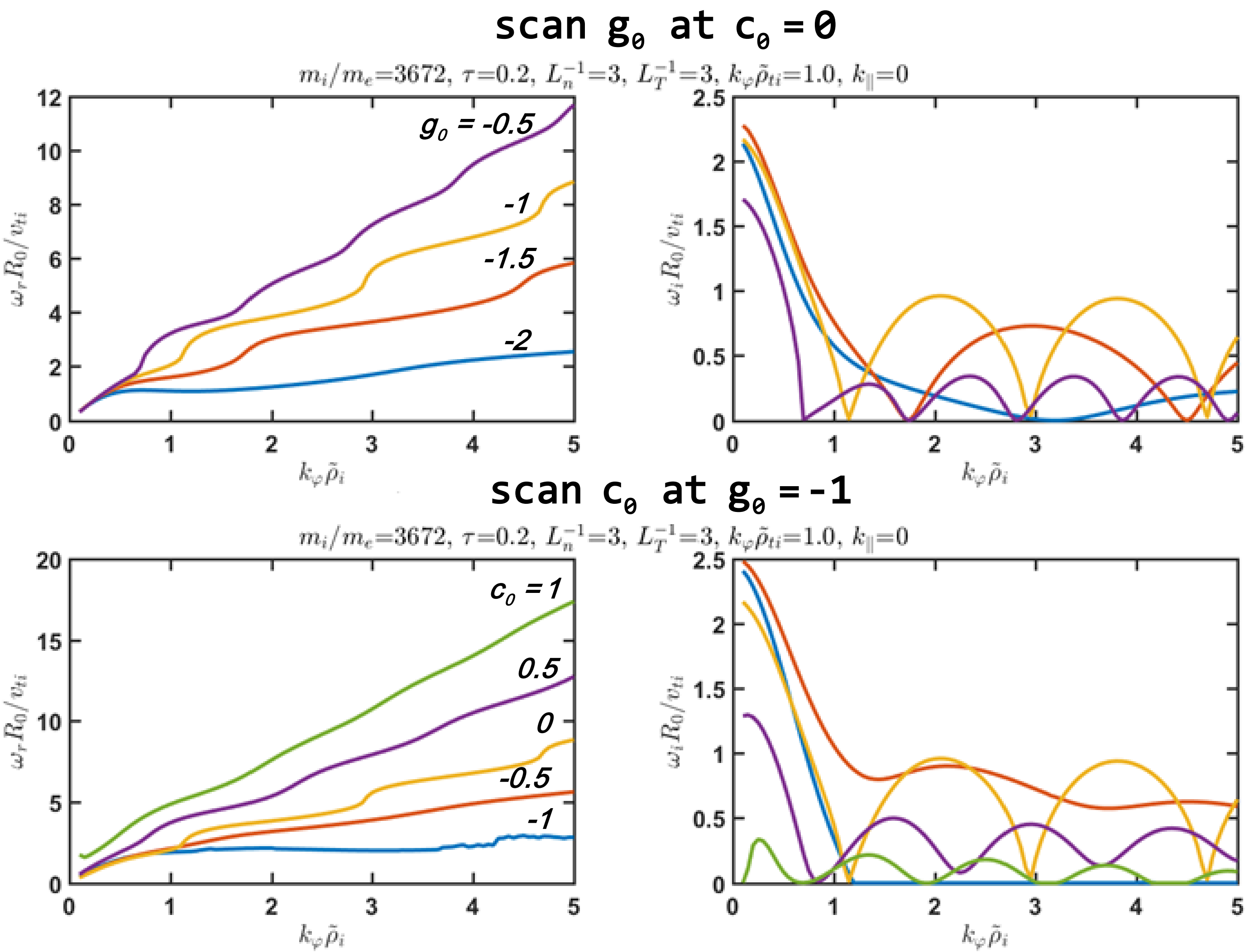

Magnetic curvature and gradient have important influences on the growth rate of drift wave.

Comparison between gkd1d simulation results and dispersion relation.

$$m_i / m_e = 3672,\ \tau=0.2,\ c_0 = 0.03053,\ g_0 = -1.2709,\ L_{ni}^{-1} = 4,\ L_{ne}^{-1} = 4,\ L_{Ti}^{-1} = 4,\ L_{Te}^{-1} = 4$$

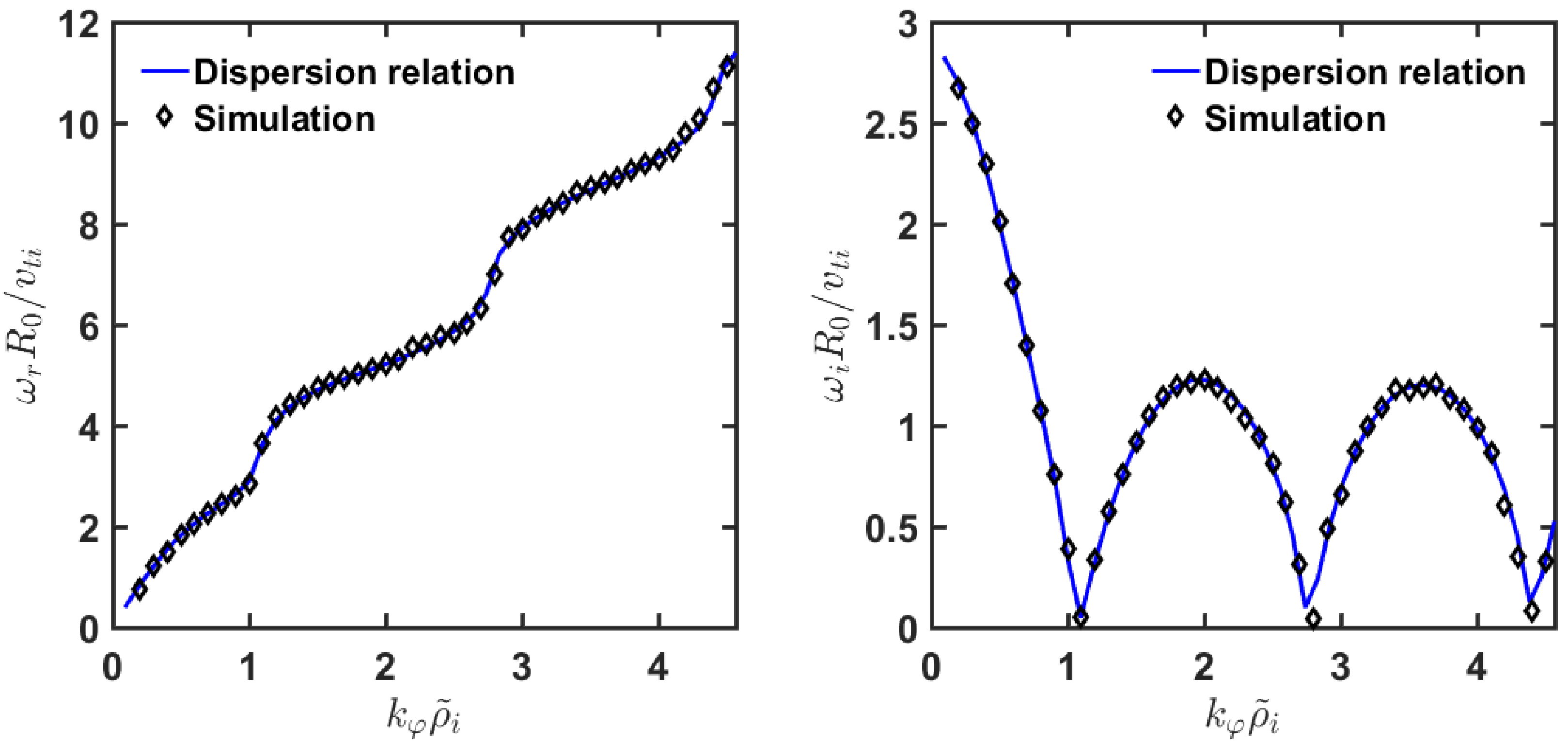

Benchmark tests of Program gkd1d at slab limit show good agreement with 0D theoretical DR results (error <1%).

5. The simulation domain for CORE and SOL

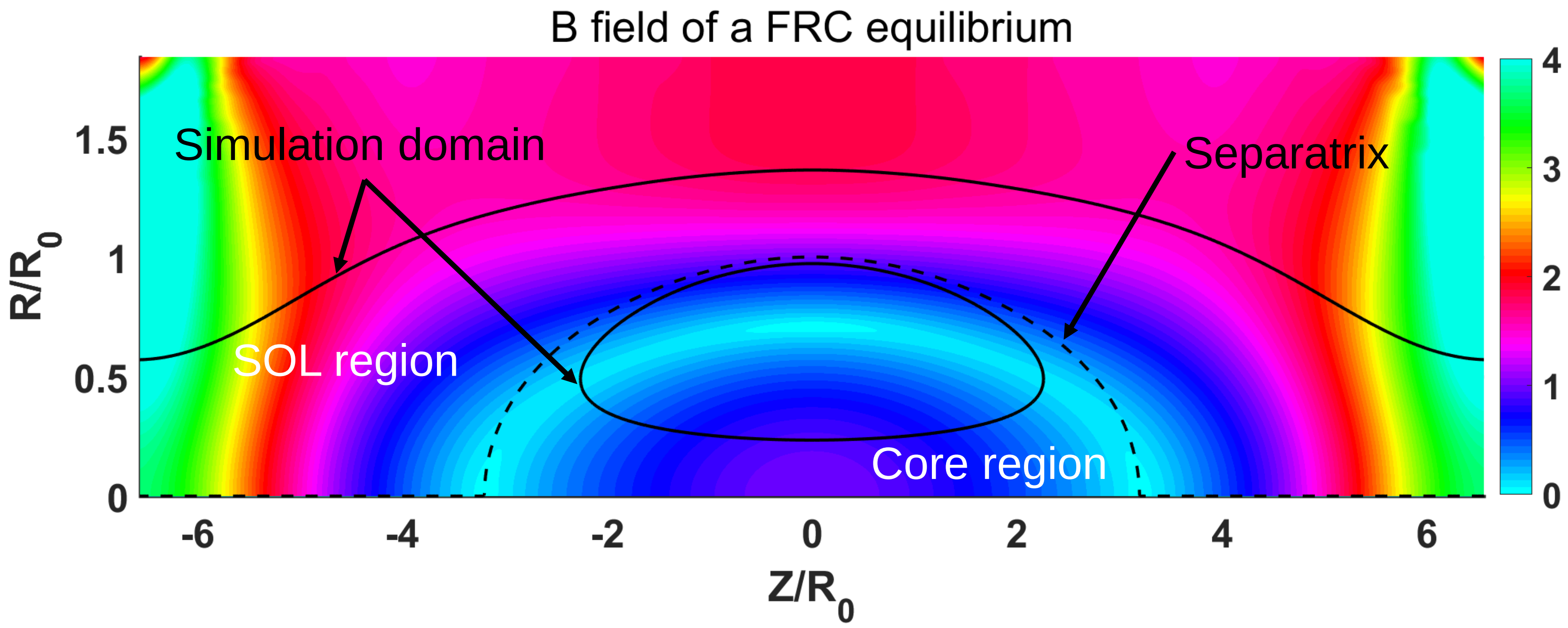

We simulate the above two flux surfaces use 1D model, with typical FRC Core and SOL parameters.

5. Input parameters for CORE region

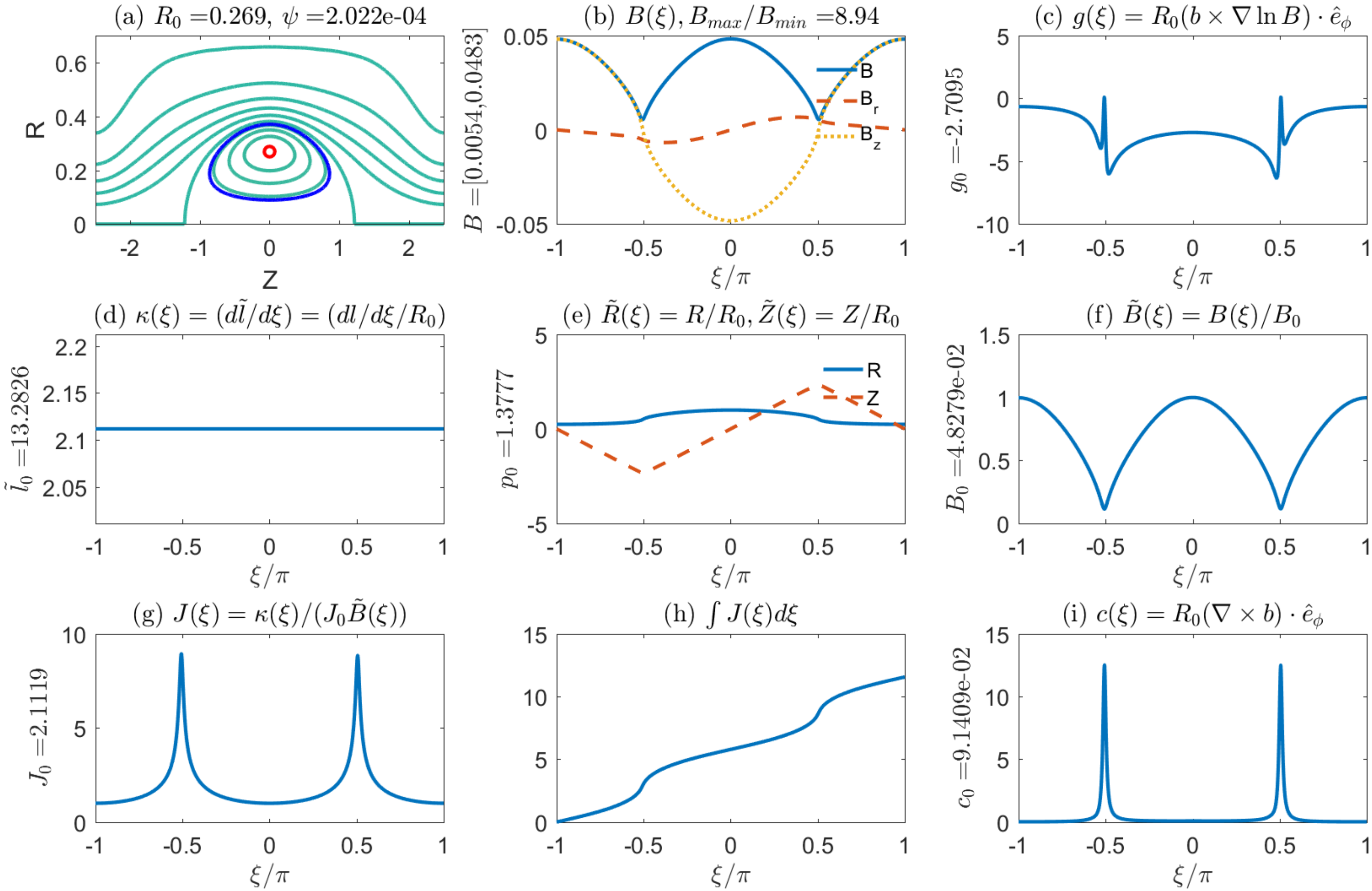

5. No linear drift wave instability in core region

Simulation result in core region of FRC, using $L_n^{-1} = L_T^{-1} = 2$.

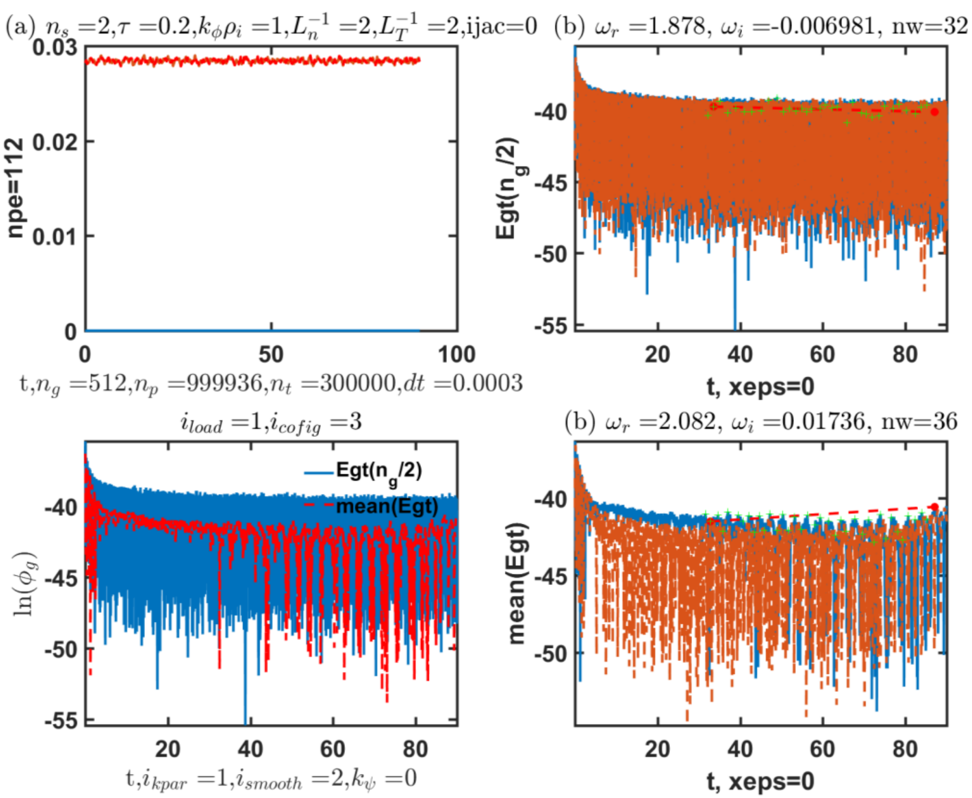

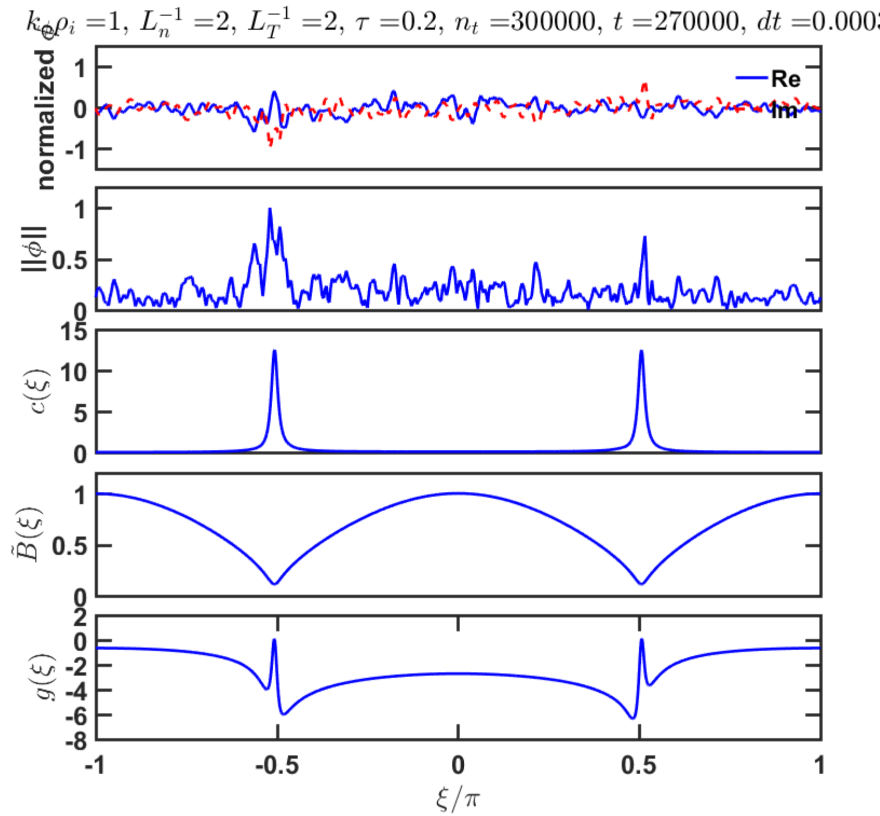

The perturbed electro-static field and potential in core region is stable (no increasement) in our simulation, in agreement with Fulton 2016.

5. Input parameters for SOL region

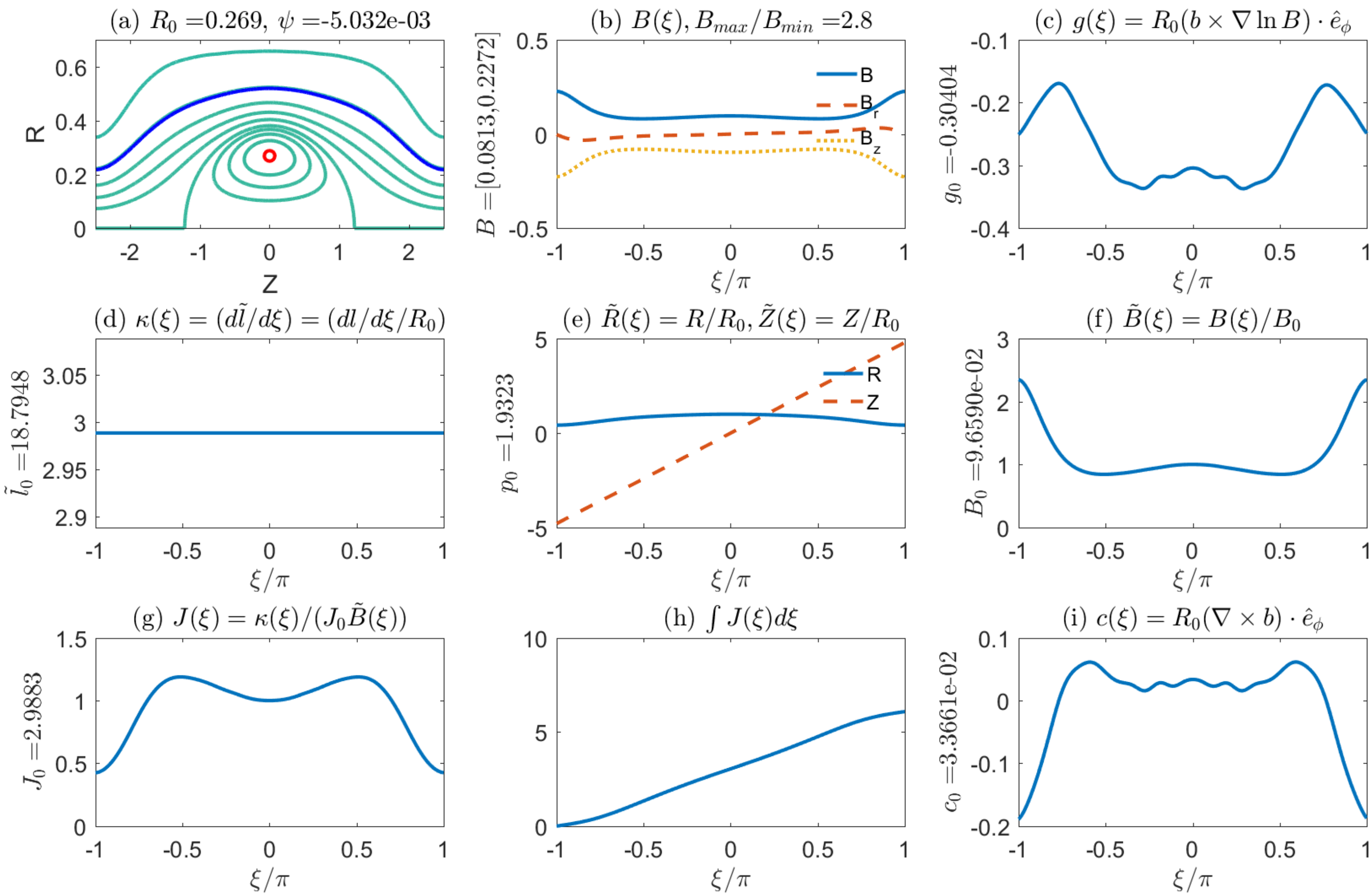

5. Linear drift wave instability in SOL region

Simulation result in SOL of FRC, using $L_n^{-1} = L_T^{-1} = 4.1$.

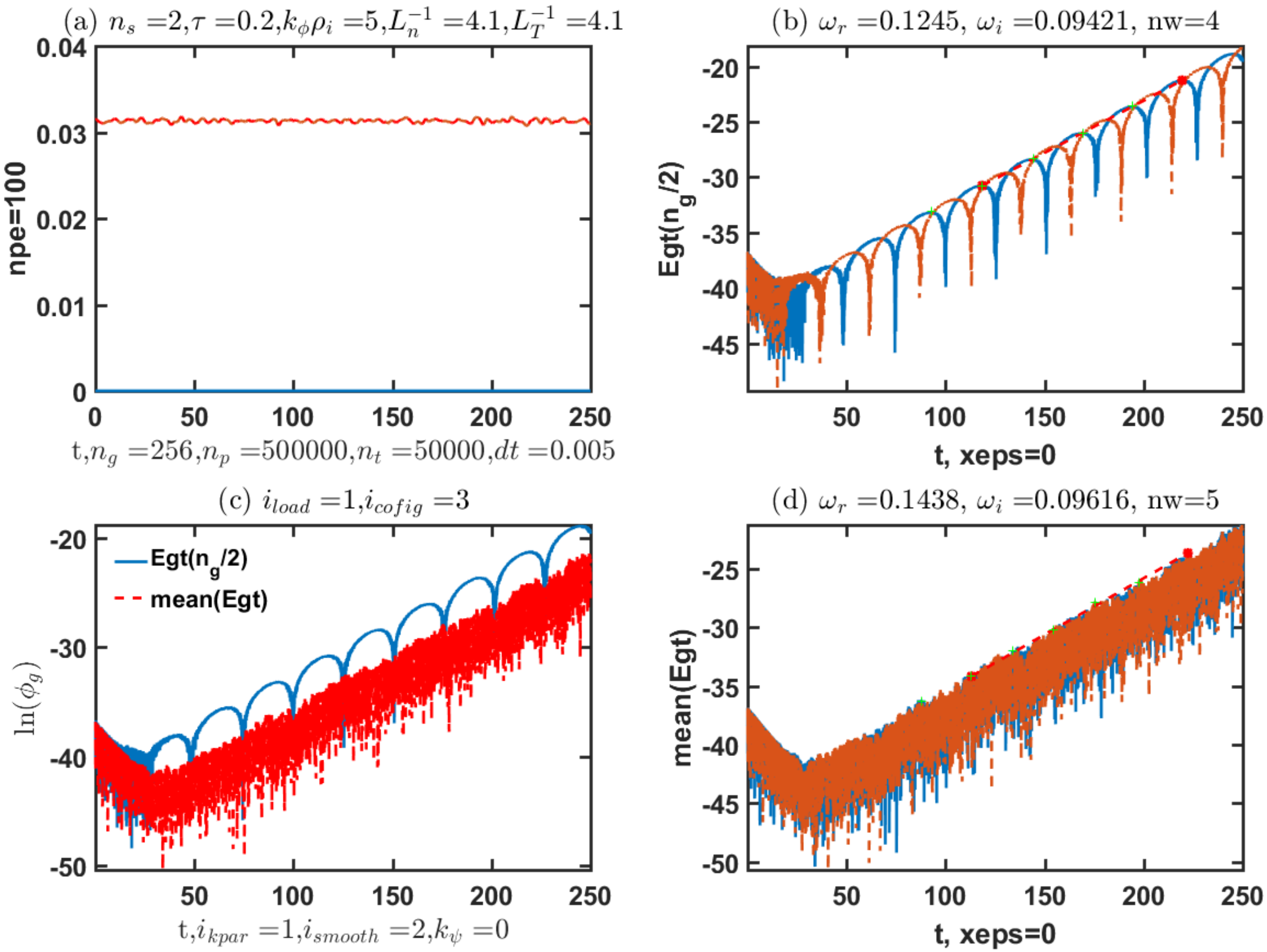

The increasement (mode unstable) of perturbed electro-static field and potential in SOL region are indeed observed.

5. Mode structure in SOL region

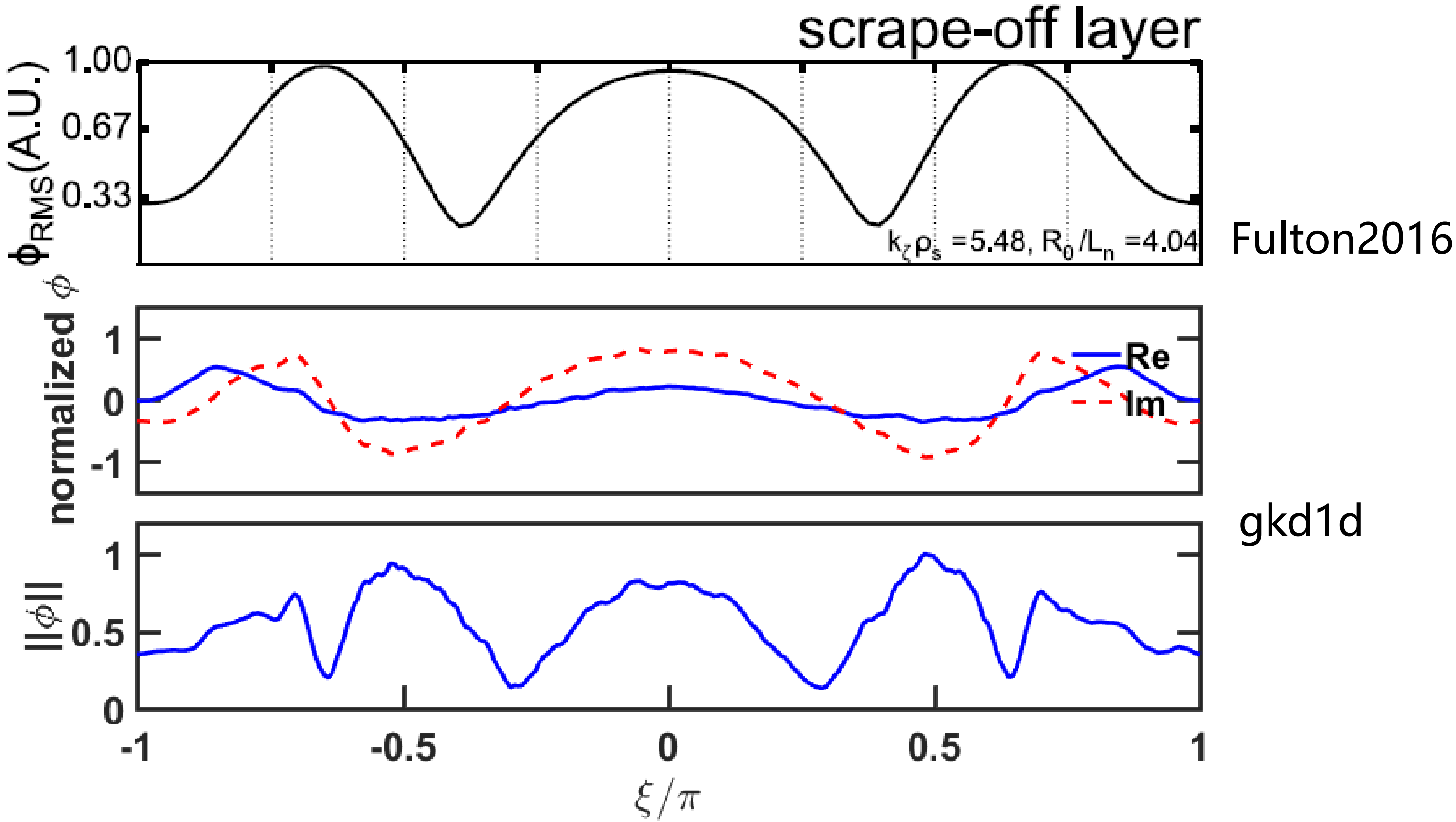

For both the real and the imaginary parts of phi, the qualitative feature are in agreement with Fulton 2016. However, the RMS value shows an additional feature, probably due to the interference between the real part and the imaginary part. More comparison and analyzation need to be done.

5. Frequency and growth rate of linear drift mode

Scan $k_{\varphi}\rho_s$, and compare with previous reports.

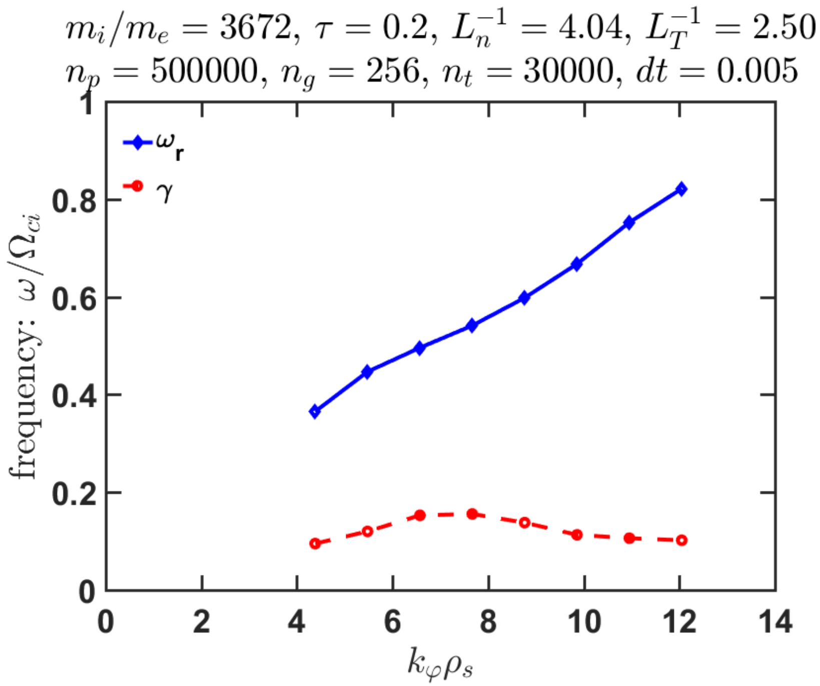

Present work: 1D simulation with gkd1d

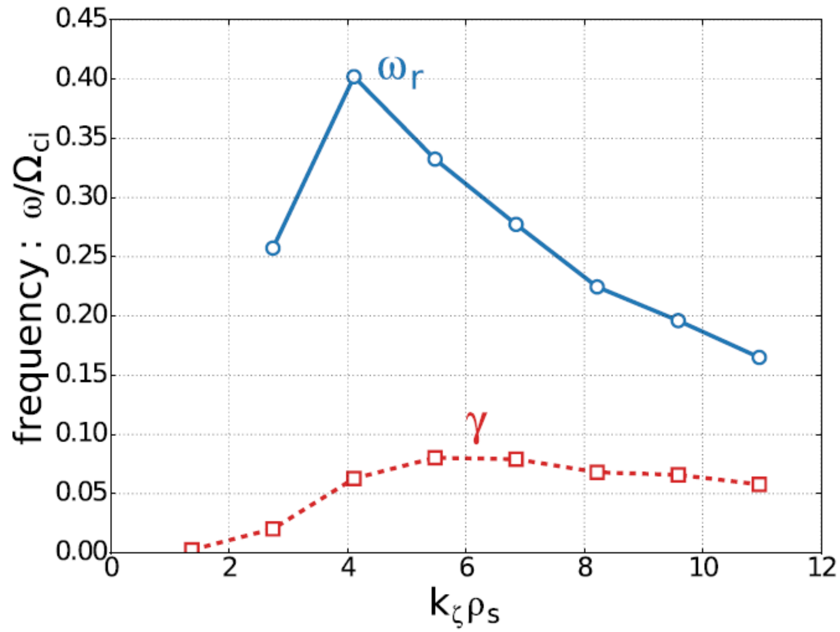

Simulation results with GTC from Fulton 2016a

The growth rate of linear drift mode show quantitatively agreement with Fulton's reports. However, the result frequency of our simulation shows qualitatively differences to them, which should be analyzed and discussed.

5. Frequency and growth rate of linear drift mode

Relationship of linear growth rate with instability drive $L_n^{-1} = L_T^{-1}$ for different $k_\varphi \rho_s$

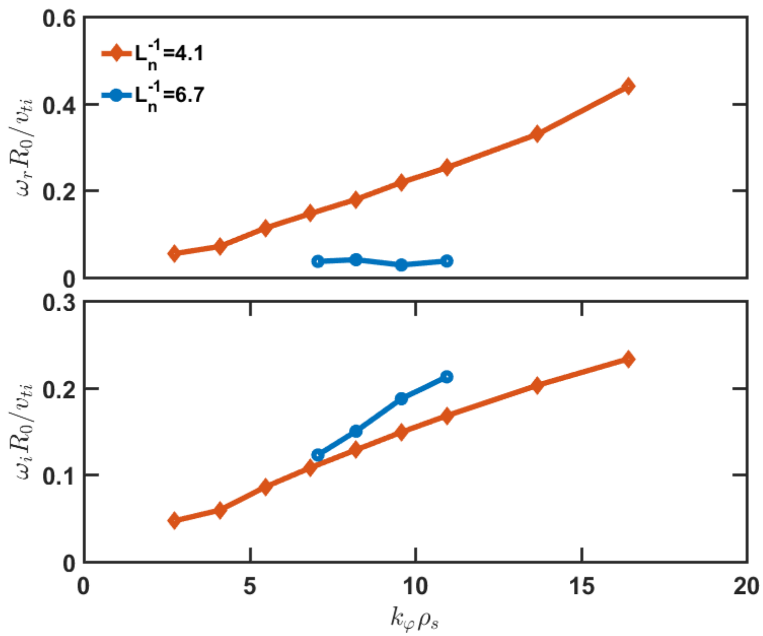

Present work: 1D simulation with gkd1d

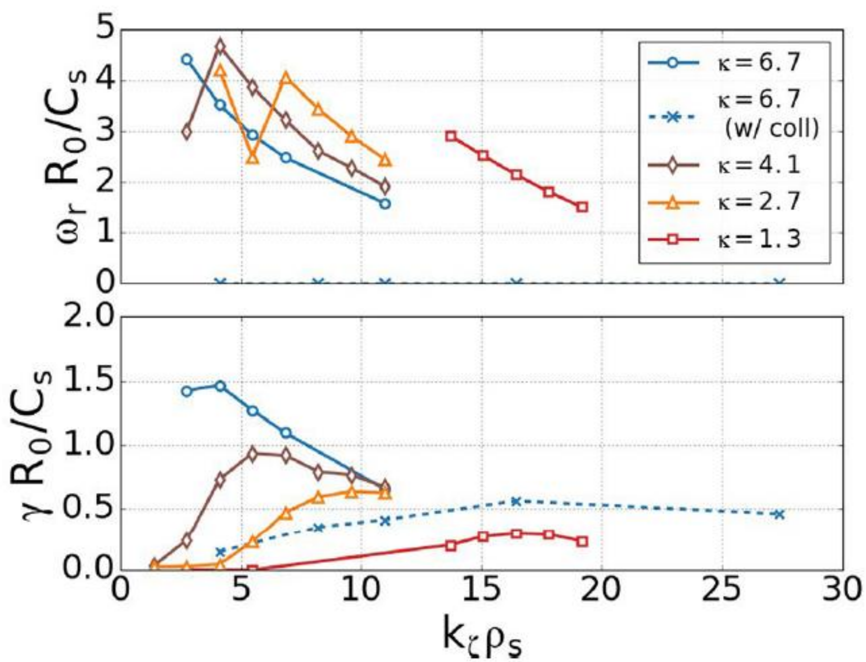

Simulation results with GTC from Lau 2017

The result frequency and growth rate of our simulation shows qualitatively differences to Fulton's reports, which should be analyzed and discussed.

6. Summary

1. The dispersion relation of the linear electrostatic drift mode is studied in a 0D model. Effects of the magnetic field curvature and gradient on the drift wave growth rate are discussed.

2. Simulation code, gkd1d, of 1D linear electrostatic drift mode has been accomplished, and the benchmark shows its correctness.

3. Our simulation shows no electrostatic drift wave instability in the core region of FRC, in agreement with previous investigations.

4. Simulation of the SOL qualitative agreement with previous investigation on the growth rate, however dramatic discrepancy on the real frequency, which motivates a further investigation.